The Evolution of [{$Ph_2P(CH_2)_nPPh_2$}Pt(μ-S)$_2$Pt{$Ph_2P(CH_2)_nPPh_2$}] ($n = 2$, 3) Metalloligands in Protic Acids: A Cascade of Sequential Reactions

Rubén Mas-Ballesté,[a] Gabriel Aullón,[a] Paul A. Champkin,[b] William Clegg,[b] Claire Mégret,[a] Pilar González-Duarte,*[a] and Agustí Lledós*[a]

Abstract: Given the nucleophilicity of the {Pt_2S_2} ring, the evolution of [Pt_2(μ-S)$_2$(P∩P)$_2$] (P∩P = 1,2-bis(diphenylphosphino)ethane (dppe), 1,3-bis(diphenylphosphino)propane (dppp)) metalloligands in the presence of the simplest electrophilic species, the proton, has been studied. Combined use of experimental and theoretical data has allowed the whole set of reactions ensuing the protonation of the {Pt_2S_2} core to be established. The titration of [Pt_2(μ-S)$_2$(P∩P)$_2$] with HCl or $HClO_4$ was monitored mainly by $^{31}P\{^1H\}$ NMR and mass techniques. Characterization of all the species involved was completed with the determination of the crystal structure of [Pt(SH)$_2$(P∩P)], for dppe and dppp, and [Pt_3(μ$_3$-S)$_2$(dppp)$_3$](PF_6)$_2$. The first protonation step of the {Pt_2S_2} core leads to the stable [Pt_2(μ-S)(μ-SH)(P∩P)$_2$]$^+$ complex, but the second step implies disintegration of the ring, thus giving rise to various mononuclear species. The subsequent evolution of some of these species allows regeneration of [Pt_2(μ-S)(μ-SH)(P∩P)$_2$]$^+$, evidencing the cyclic nature of this process. Whereas the reaction pathway is essentially common for both phosphine ligands, dppe and dppp, the different coordinating ability of Cl^- or ClO_4^- determines the nature of the final products, [$PtCl_2$(P∩P)], [Pt_3(μ$_3$-S)$_2$(P∩P)$_3$]Cl_2 or [Pt_3(μ$_3$-S)$_2$(P∩P)$_3$](ClO_4)$_2$. DFT calculations have corroborated the thermodynamic feasibility of the reactions proposed on the basis of experimental data.

Keywords: nucleophilicity · platinum · protonation · S ligands

Introduction

The high nucleophilicity of the bridging sulfido ligands in the {Pt_2S_2} core accounts for the exceptional chemical features of complexes of the formula [$L_2Pt(\mu\text{-}S)_2PtL_2$].[1] In this context, their ability to act as metalloligands in the assembly of a diverse range of sulfido-bridged higher nuclearity aggregates has prompted most of the research into such compounds in recent years.[2] In addition to the reaction of [$L_2Pt(\mu\text{-}S)_2PtL_2$] with metal substrates, that with organic electrophilic agents such as $PhCH_2Br$,[3] CH_3I,[4] and CH_2Cl_2[5] has also been described. As regards the last of these, we recently reported the reaction pathways by which the complexes [Pt_2(μ-S)$_2$(P∩P)$_2$] (P∩P = 1,2-bis(diphenylphosphino)ethane (dppe) **1a**; 1,3-bis(diphenylphosphino)propane (dppp) **1b**) react with CH_2Cl_2.[6] The observed dependence on the nature of the diphosphine ligands, together with the high number and different natures of the species characterized, provided evidence for the rich and diverse chemistry of the {Pt_2S_2} core and encouraged us to extend the nucleophilicity studies to the simplest electron-acceptor species, the proton.

Herein, we explore the reactivity of **1a** and **1b** towards two protic acids, HCl and $HClO_4$, which differ in the coordination ability of the corresponding conjugate bases. Thus, the first and second protonation steps of the {Pt_2S_2} core in the previous complexes and particularly the multistage pathways following cleavage of the {$Pt_2(\mu\text{-}SH)_2$} ring are discussed in detail. Verification of the proposed reaction pathways, shown in Schemes 1 and 2, has required the synthesis and characterization of the mononuclear complexes [Pt(SH)$_2$(P∩P)], (P∩P = dppe **4a**; dppp **4b**), which are transient species resulting from this cleavage. Remarkably, in the presence of HCl and $HClO_4$, **4a** and **4b** spontaneously evolve to the corresponding dinuclear monoprotonated species [Pt_2(μ-S)(μ-SH)(P∩P)$_2$]$^+$ (P∩P = dppe, **2a**, or dppp, **2b**), thus accounting for the cyclic nature of the reactions of **1a** and **1b** with protic acids.

An additional interest in several complex species reported here arises from their relevance to the process of removal of sulfur as SH_2 from petroleum feedstocks, known as hydrodesulfurization (HDS). Thus, the previously characterized complex [$(PPh_3)_2Pt(\mu\text{-}S)_2Pt(PPh_3)_2$] (an analogue of **1a** and **1b**) is obtained as a result of the reaction of [$Pt(PPh_3)_2C_2H_4$] with η^6-coordinated benzothiophene, as a model for homoge-

[a] Prof. Dr. P. González-Duarte, Prof. Dr. A. Lledós, Dipl.-Chem. R. Mas-Ballesté, Dr. G. Aullón, Dipl.-Chem C. Mégret
Departament de Química
Universitat Autònoma de Barcelona
08193 Bellaterra, Barcelona (Spain)
Fax: (+34) 935-813-101
E-mail: Pilar.Gonzalez.Duarte@uab.es

[b] Dr. P. A. Champkin, Prof. Dr. W. Clegg
Department of Chemistry
University of Newcastle, Newcastle upon Tyne, NE1 7RU (UK)

 DOI: 10.1002/chem.200304983

neous HDS of relatively unreactive sulfur-containing species.[7] Moreover, complex species containing the Pt–SH fragment, which is present in complexes $[Pt_2(\mu\text{-}S)(\mu\text{-}SH)(P\cap P)_2]^+$ ($P\cap P$ = dppe, **2a**, or dppp, **2b**), $[Pt_2(\mu\text{-}SH)_2(P\cap P)_2]^{2+}$ ($P\cap P$ = dppe, **3a**, or dppp, **3b**) and $[Pt(SH)_2(P\cap P)]$ ($P\cap P$ = dppe, **4a**, or dppp, **4b**), have been proposed as intermediate species in HDS.[8] The fact that Pt–SH-containing species are scarce[9] and that complexes of formula $[Pt(SH)_2L_2]$ are considered as good potential catalysts in the Claus process (consisting of the oxidation of the SH_2, formed in the HDS process, to elemental sulfur),[10] provide further interest to this study.

Overall, the systematic investigation of the reactions involved in the protonation of the $\{Pt_2S_2\}$ core in the complexes $[Pt_2(\mu\text{-}S)_2(P\cap P)_2]$ (**1a** and **1b**) gives more evidence of the remarkable chemistry of the aforementioned metalloligands in the presence of electrophilic agents and shows the ease of interconversion between apparently unrelated platinum complexes containing the Pt–SH fragment.

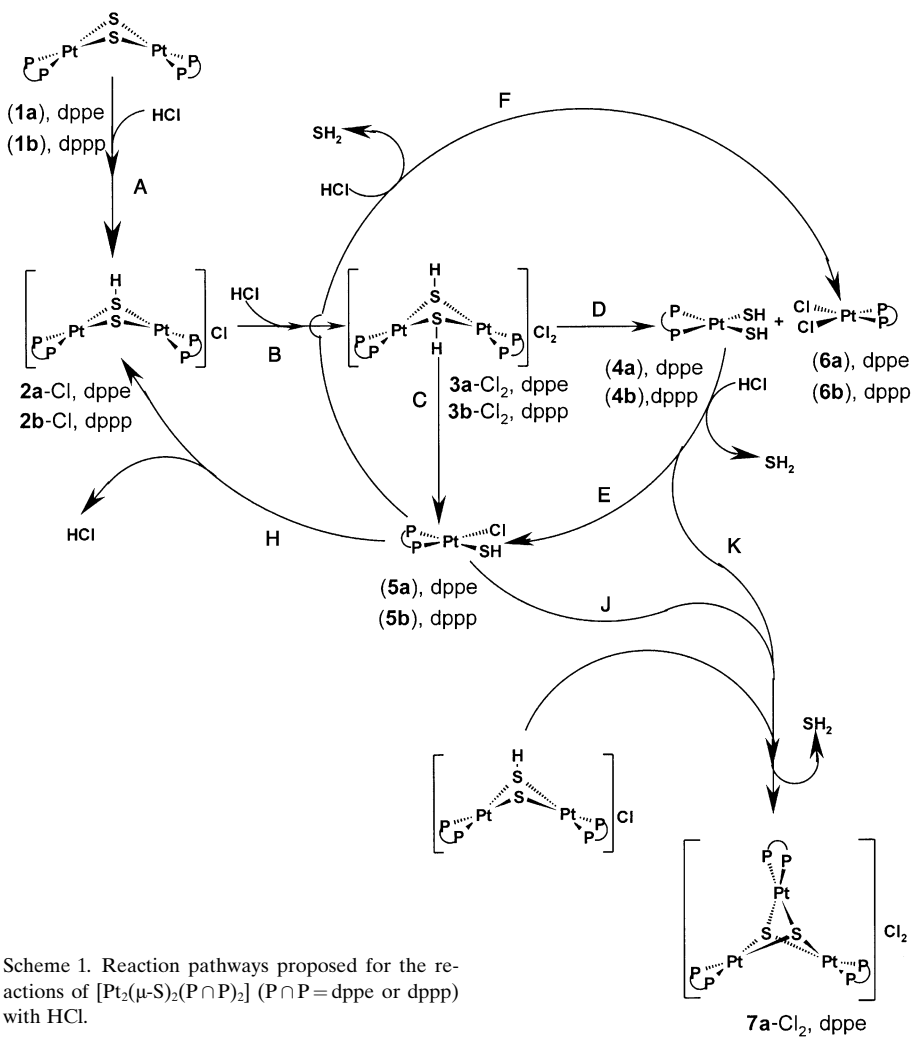

Scheme 1. Reaction pathways proposed for the reactions of $[Pt_2(\mu\text{-}S)_2(P\cap P)_2]$ ($P\cap P$ = dppe or dppp) with HCl.

Abstract in Catalan: *En base a la nucleofilicitat de l'anell $\{Pt_2S_2\}$, s'ha estudiat l'evolució dels metal·lolligands $[Pt_2(\mu\text{-}S)_2(P\cap P)_2]$ ($P\cap P$ = dppe, dppp) envers l'electròfil més senzill, el protó. La combinació de dades experimentals i teòriques ha permès establir el conjunt de reaccions que es deriven de la protonació de l'anell $\{Pt_2S_2\}$. El seguiment de la valoració de $[Pt_2(\mu\text{-}S)_2(P\cap P)_2]$ amb HCl o $HClO_4$ s'ha efectuat essencialment per tècniques de RMN de $^{31}P\{^1H\}$ i d'espectrometria de masses. La caracterització de totes les espècies implicades s'ha completat amb la determinació de l'estructura cristal·lina de $[Pt(SH)_2(P\cap P)]$, per dppe i dppp, i $[Pt_3(\mu_3\text{-}S)_2(dppp)_3](PF_6)_2$. La primera protonació de l'anell $\{Pt_2S_2\}$ dóna lloc a un complex estable, $[Pt_2(\mu\text{-}S)(\mu\text{-}SH)(P\cap P)_2]^+$, però la segona té com a conseqüència la desintegració de l'esmentat anell, originant la formació de diverses espècies mononuclears. L'evolució posterior d'algunes d'aquestes espècies permet la regeneració de $[Pt_2(\mu\text{-}S)(\mu\text{-}SH)(P\cap P)_2]^+$, evidenciant així la naturalesa cíclica del procés. Si bé, qualitativament, el camí de reacció és comú per les dues fosfines, dppe i dppp, la diferent capacitat coordinant de Cl^- o ClO_4^- determina la naturalesa dels productes finals, $[PtCl_2(P\cap P)]$, $[Pt_3(\mu_3\text{-}S)_2(P\cap P)_3]Cl_2$ o $[Pt_3(\mu_3\text{-}S)_2(P\cap P)_3](ClO_4)_2$. Els càlculs teòrics (DFT) han permès establir la viabilitat termodinàmica dels processos proposats en base a les dades experimentals.*

Results and Discussion

General description of the evolution of the complexes $[Pt_2(\mu\text{-}S)_2(P\cap P)_2]$ ($P\cap P$ = dppe, dppp) in the presence of HCl and $HClO_4$: The reaction pathways proposed for the reactions of $[Pt_2(\mu\text{-}S)_2(P\cap P)_2]$ (**1**) with HCl (Scheme 1) and $HClO_4$ (Scheme 2) are based on the experimental data summarized in Tables 1 and 2.

The first information on these reactions was obtained by monitoring the $^{31}P\{^1H\}$ NMR parameters of the species present in solution after controlled addition of HCl to **1** in acetonitrile. Up to one equivalent of protons per mole of $[Pt_2(\mu\text{-}S)_2(P\cap P)_2]$, the addition of HCl led to the immediate formation of $[Pt_2(\mu\text{-}S)(\mu\text{-}SH)(P\cap P)_2]Cl$, **2**-Cl, which are stable in solution and have been structurally characterized in the solid phase as the perchlorate salts, **2**-ClO_4.[11] Subsequent additions of HCl had a small effect, until a significant excess of protons was added with respect to the stoichiometric ratio required to obtain the corresponding diprotonated complexes $[Pt_2(\mu\text{-}SH)_2(P\cap P)_2]^{2+}$ (**3**). After this, the excess of protons produced a decrease in the concentration of **2**-Cl and the concomitant appearance of the corresponding mononuclear species $[PtCl_2(P\cap P)]$ (**6**). For both **1a** and **1b**, the concentration of $[PtCl_2(P\cap P)]$ formed

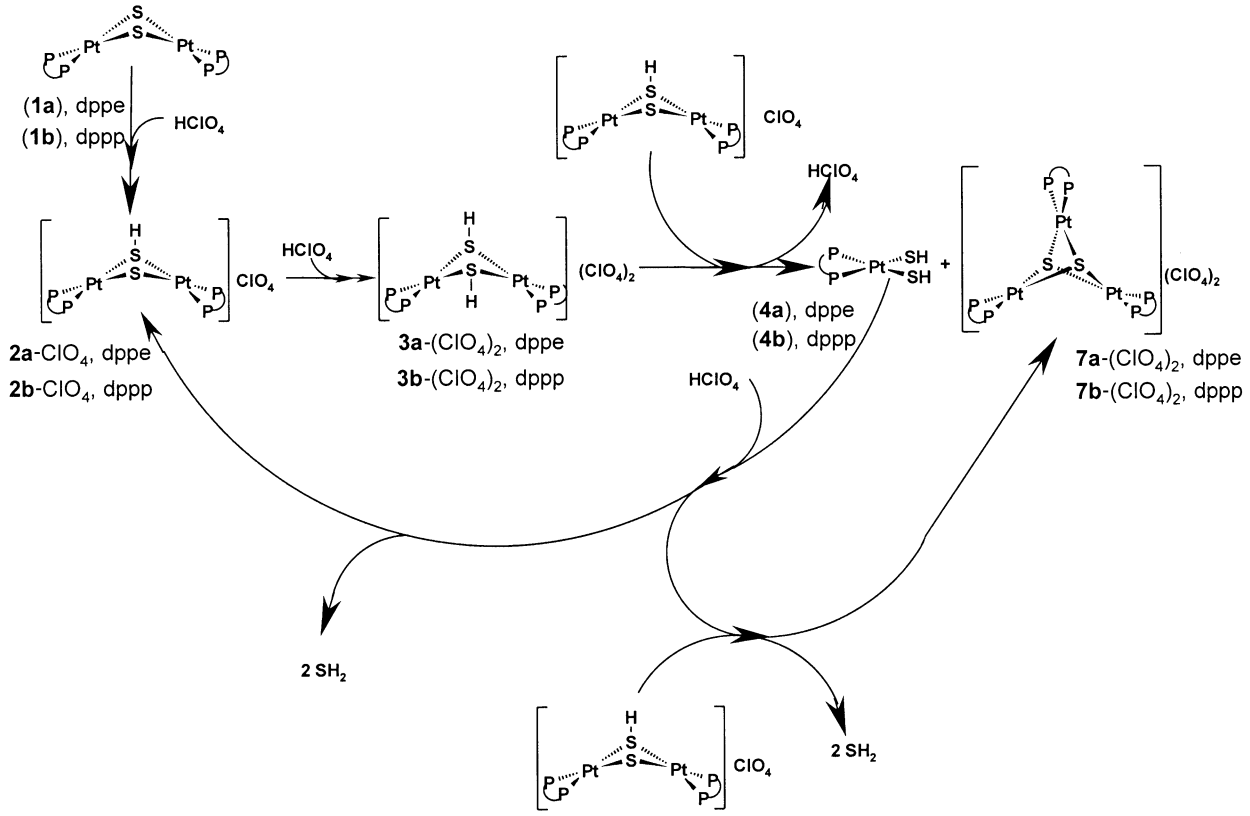

Scheme 2. Reaction pathways proposed for the reactions of $[Pt_2(\mu\text{-}S)_2(P\cap P)_2]$ ($P\cap P$ = dppe or dppp) with $HClO_4$.

Table 1. Identification of the complex species formed throughout different processes as deduced by $^{31}P\{^1H\}$ NMR data.

Experiment	Acid added	Amount of acid added (equiv)	Species detected in solution by $^{31}P\{^1H\}$ NMR	
			$P\cap P$ = dppe	$P\cap P$ = dppp
Titration of **1** with acid	HCl	2	**2a**-Cl + **6a** (minor)	**2b**-Cl + **6b** (minor)
		16	**2a**-Cl + **6a**	**2b**-Cl + **6b** (minor)
		50	**6a**	**2b**-Cl + **6b**
	$HClO_4$	5	**2a**-ClO_4 + (**7a**)$(ClO_4)_2$ (minor)	**2b**-ClO_4
		50	**2a**-ClO_4 + **7a**-$(ClO_4)_2$	**2b**-ClO_4
		75	**7a**-$(ClO_4)_2$	**2b**-ClO_4
		150	**7a**-$(ClO_4)_2$	**2b**-ClO_4 + **7b**-$(ClO_4)_2$ (minor)
Titration of **4** with acid	HCl	25	**2a**-Cl + **7a**-Cl_2 + **6a** (minor)	**2b**-Cl + **6b** (minor)
		50	**6a** + **7a**-Cl_2	**2b**-Cl + **6b**
		75	**6a**	**2b**-Cl + **6b**
	$HClO_4$	2	**2a**-ClO_4 + **7a**-$(ClO_4)_2$ (minor)	**2b**-ClO_4
		5	**2a**-ClO_4 + **7a**-$(ClO_4)_2$	**2b**-ClO_4
		25	**7a**-$(ClO_4)_2$	**2b**-ClO_4
Evolution of **2** in the presence of acid after 1 week	HCl	4	**2a**-Cl + **7a**-Cl_2 + **6a**	**2b**-Cl + **6b**
	$HClO_4$	4	**7a**-$(ClO_4)_2$	no reaction
2 + **6**	–	–	No reaction	no reaction
6 + NaSH (1:1)	–	–	**2a**-Cl + **4a** (minor)	**2b**-(Cl) + **4b** (minor)

was directly related to the amount of HCl added but, for the same amount, the $[PtCl_2(P\cap P)]$ to $[Pt_2(\mu\text{-}S)(\mu\text{-}SH)(P\cap P)_2]Cl$ molar ratio obtained was always greater for dppe than for dppp. After one week, in the case of **2a**-Cl only, the addition of up to approximately four equivalents of acid led to the formation of $[Pt_3(\mu_3\text{-}S)_2(dppe)_3]Cl_2$, **7a**-$Cl_2$, whose X-ray crystal structure and NMR parameters have already been reported.[2e]

Whereas the addition of one equivalent of $HClO_4$ per mole of **1** in acetonitrile caused the immediate formation of **2**-ClO_4, an excess of $HClO_4$ gave rise to the concomitant appearance of the corresponding trinuclear complex $[Pt_3(\mu_3\text{-}S)_2(P\cap P)_3]^{2+}$ (**7**). This occurred in a substantial amount for **7a**-$(ClO_4)_2$, but it required a great excess of acid for **7b**-$(ClO_4)_2$. The crystal structure of **7a**-Cl_2 is known[2e] and that of **7b**-$(PF_6)_2$ is reported here.

Consideration of both sets of data and complementary information (described below) allowed us to deduce that the addition of protons to **2** had caused them to evolve to the corresponding diprotonated complexes **3**, which were of an

Table 2. ESMS and NMR data for complexes **1**, **2**, **4**, **6** and **7**.

Compound	*m*/*z*	Calculated MW	$\delta(^{31}P)$ [ppm][a]	$^{1}J_{Pt,P}$ (Hz)
$[Pt_2(\mu\text{-}S)_2(dppe)_2]$ (**1a**)	1251.7[b]	1251[b]	40.5	2740
$[Pt_2(\mu\text{-}S)_2(dppp)_2]$ (**1b**)	1279.7[b]	1279[b]	−0.1	2615
$[Pt_2(\mu\text{-}S)(\mu\text{-}SH)(dppe)_2]^+$ (**2a**)	1251.7	1251	45.4[c]	3110[c]
$[Pt_2(\mu\text{-}S)(\mu\text{-}SH)(dppp)_2]^+$ (**2b**)	1279.7	1279	−0.8[c]	2965[c]
$[Pt(SH)_2(dppe)]$ (**4a**)[d]	626.2	659	48.5	2883
$[Pt(SH)_2(dppp)]$ (**4b**)[e]	640.1	673	−1.3	2768
$[PtCl_2(dppe)]$ (**6a**)	–		43.4	3610
$[PtCl_2(dppp)]$ (**6b**)	–		−3.7	3408
$[Pt_3(\mu_3\text{-}S)_2(dppe)_3]^{2+}$ (**7a**)	921.4[f]	1844	38.3	3248
$[Pt_3(\mu_3\text{-}S)_2(dppp)_3]^{2+}$ (**7b**)	943.0[f]	1886	–10.8[g]	3016[g]

[a] In $[D_6]$DMSO. [b] $m/e = M+1$. [c] Apparent parameters at room temperature. [d] ^{1}H NMR parameters for **4a**: $\delta(^1H\text{-}S) = -0.82$ ppm; $^2J_{H,Pt} = 51.7$ Hz; $^3J_{H,P(trans)} = 10.8$ Hz, $^3J_{H,P(cis)} = 3.5$ Hz. [e] ^{1}H NMR parameters for **4b**: $\delta(^1H\text{-}S) = -1.00$ ppm; $^2J_{H,Pt} = 48.5$ Hz; $^3J_{H,P(trans)} = 7.2$ Hz. [f] $m/e = M/2$. [g] ^{31}P NMR parameters from the computer simulation for $[Pt_3(\mu_3\text{-}S)_2(dppp)_3]^{2+}$: $\delta(^{31}P) = -10.7$ ppm; $^1J_{Pt,P} = 3016$ Hz; $^2J_{Pt,Pt} = 705$ Hz; $^3J_{Pt,P} < 10$ Hz; $^4J_{P,P} < 10$ Hz.

elusive nature. The sequence of protonation reactions with HCl is given in **A** and **B**.

$$[Pt_2(\mu\text{-}S)_2(P\cap P)_2]\ (\mathbf{1}) + HCl \rightarrow [Pt_2(\mu\text{-}S)(\mu\text{-}SH)(P\cap P)_2]Cl\ (\mathbf{2}\text{-}Cl) \qquad (\mathbf{A})$$

$$[Pt_2(\mu\text{-}S)(\mu\text{-}SH)(P\cap P)_2]Cl\ (\mathbf{2}\text{-}Cl) + HCl \rightarrow [Pt_2(\mu\text{-}SH)_2(P\cap P)_2]Cl_2\ (\mathbf{3}\text{-}Cl_2) \qquad (\mathbf{B})$$

The fact that this second protonation step **B**, unlike the first one **A**, required a significant excess of protons with respect to the stoichiometric ratio indicates that the complexes $[Pt_2(\mu\text{-}S)_2(P\cap P)_2]$ (**1**) are stronger bases than their monoprotonated counterparts $[Pt_2(\mu\text{-}S)(\mu\text{-}SH)(P\cap P)_2]^+$ (**2**), the pK_a values of **2** on the aqueous scale falling in the range 7–9.[11] Moreover, the basicity of **2** is dependent on the nature of the diphosphine ligand, being higher for dppe than for dppp. Overall, the ease of decomposition of **3** impaired their observation in solution, but could account for the different complexes obtained spontaneously as a result of the disintegration of the $\{Pt_2(\mu\text{-}SH)_2\}$ core in these species. The cascade of reactions following this disintegration depends on the nature of the diphosphine ligands and on the coordinating ability of the conjugate base, Cl^- or ClO_4^-, of the acid added. Thus, the sequence of reactions resulting from the addition of HCl to complexes **1** will be described first (Scheme 1), and this will be followed by that involving the addition of $HClO_4$ (Scheme 2).

Following the previous assumption, the reaction between HCl and **2** entails formation of the $\{Pt_2(\mu\text{-}SH)_2\}$ ring, which then cleaves either symmetrically (reaction **C**), affording two equivalents of $[PtCl(SH)(P\cap P)]$ (**5**), or asymmetrically (reaction **D**), leading to a mixture of $[PtCl_2(P\cap P)]$ and $[Pt(SH)_2(P\cap P)]$, that is **4** and **6**.

$$[Pt_2(\mu\text{-}SH)_2(P\cap P)_2]Cl_2\ (\mathbf{3}\text{-}Cl_2) \rightarrow 2\ [PtCl(SH)(P\cap P)]\ (\mathbf{5}) \qquad (\mathbf{C})$$

$$[Pt_2(\mu\text{-}SH)_2(P\cap P)_2]Cl_2\ (\mathbf{3}\text{-}Cl_2) \rightarrow [Pt(SH)_2(P\cap P)]\ (\mathbf{4}) + [PtCl_2(P\cap P)]\ (\mathbf{6}) \qquad (\mathbf{D})$$

The presence of an excess of HCl in solution, which is required for the formation of the diprotonated cations **3**, causes protonation of SH^- and thus its replacement by Cl^- in **4** and **5** (reactions **E** and **F**), as well as the wholesale displacement of these reactions toward the formation of the corresponding compounds **6**, both already known[12] and thus easily identified in solution.[6]

$$[Pt(SH)_2(P\cap P)]\ (\mathbf{4}) + HCl \rightarrow [PtCl(SH)(P\cap P)]\ (\mathbf{5}) + H_2S \qquad (\mathbf{E})$$

$$[PtCl(SH)(P\cap P)]\ (\mathbf{5}) + HCl \rightarrow [PtCl_2(P\cap P)]\ (\mathbf{6}) + H_2S \qquad (\mathbf{F})$$

To verify these reactions we carried out the synthesis and characterization of complexes **4** (described below) and monitored their reactivity towards HCl and $HClO_4$ by a procedure similar to that followed for **1**. Addition of a significant excess of HCl to **4** in acetonitrile yielded **6**, and thus confirmed reactions **E** and **F**. On the other hand, when the amount of HCl added was limited to a smaller excess, complexes **4** spontaneously evolved to **2**, which could occur either directly (reaction **G**) or in two steps (reactions **E** and **H**) through the intermediate species **5**.

$$2\,[Pt(SH)_2(P\cap P)]\ (\mathbf{4}) + HCl \rightarrow [Pt_2(\mu\text{-}S)(\mu\text{-}SH)(P\cap P)_2]Cl\ (\mathbf{2}\text{-}Cl) + 2\,H_2S \qquad (\mathbf{G})$$

$$2\,[PtCl(SH)(P\cap P)]\ (\mathbf{5}) \rightarrow [Pt_2(\mu\text{-}S)(\mu\text{-}SH)(P\cap P)_2]Cl\ (\mathbf{2}\text{-}Cl) + HCl \qquad (\mathbf{H})$$

This last reaction could account for the spontaneous dimerization of **5** and thus for our unsuccessful attempts to detect these species. To obtain evidence for the two-step mechanism, the reaction of $[PtCl_2(P\cap P)]$ (**6**), with $NaSH\cdot H_2O$ in approximately a 1:1 molar ratio was carried out. This resulted in the formation of **2**-Cl in high yield and thus indicated that reaction **H** is feasible under the present experimental conditions. However, theoretical calculations on both processes, **G** and **H**, described below, strongly suggest that reaction **G** is more favorable than **H**.

Overall, the reaction of complexes $[Pt_2(\mu\text{-}S)_2(P\cap P)_2]$ (**1**) with HCl in excess consists of a cyclic process, where the monoprotonated species $[Pt_2(\mu\text{-}S)(\mu\text{-}SH)(P\cap P)_2]^+$ (**2**) initially formed evolves to the new species $[Pt(SH)_2(P\cap P)]$ (**4**), which in turn affords the initial complexes **2**-Cl. However, the concomitant formation of unreactive species, such as $[PtCl_2(P\cap P)]$ (**6**), under the present experimental conditions limits the cyclic process. An additional dead end, for $P\cap P =$ dppe only, is the formation of the trinuclear complex $[Pt_3(\mu_3\text{-}S)_2(dppe)_3]^{2+}$ (**7a**). It was also observed that the formation of **7a**-Cl_2, as well as **7a**-$(ClO_4)_2$, is solvent-dependent and, in both cases, the amount formed follows the order: acetonitrile > acetone ≈ methanol > methylene chloride.

There are several possible ways for the formation of the trimetallic compound **7a**-Cl_2 to occur. According to experimental data, complexes **2a**-Cl and **6a** do not react with themselves, and thus their combination (reaction **I**) cannot be a possible source for complex **7a**-Cl_2.

$$[PtCl_2(P\cap P)]\ (\mathbf{6}) + [Pt_2(\mu\text{-}S)(\mu\text{-}SH)(P\cap P)_2]Cl\ (\mathbf{2}\text{-}Cl) \rightarrow [Pt_3(\mu_3\text{-}S)_2(P\cap P)_3]Cl_2\ (\mathbf{7}\text{-}Cl_2) + HCl \qquad (\mathbf{I})$$

Two alternative reaction pathways for the formation of **7a**-Cl_2 are given in chemical equations **J** and **K**, in which the

binuclear complexes **2** react with their mononuclear counterparts **4** or **5**.

$$[Pt(SH)_2(P\cap P)]\ (\mathbf{4}) + [Pt_2(\mu\text{-}S)(\mu\text{-}SH)(P\cap P)_2]Cl\ (\mathbf{2}\text{-}Cl) + HCl \rightarrow [Pt_3(\mu_3\text{-}S)_2(P\cap P)_3]Cl_2\ (\mathbf{7}\text{-}Cl_2) + 2\,H_2S \quad (\mathbf{J})$$

$$[PtCl(SH)(P\cap P)]\ (\mathbf{5}) + [Pt_2(\mu\text{-}S)(\mu\text{-}SH)(P\cap P)_2]Cl\ (\mathbf{2}\text{-}Cl) \rightarrow [Pt_3(\mu_3\text{-}S)_2(P\cap P)_3]Cl_2\ (\mathbf{7}\text{-}Cl_2) + H_2S \quad (\mathbf{K})$$

Another possible pathway arises from the self-combination of two equivalents of $[Pt_2(\mu\text{-}SH)_2(P\cap P)_2]Cl_2$ (**3**) (reaction **L**), which affords not only **7**-Cl_2 but also the mononuclear $[Pt(SH)_2(P\cap P)]$ (**4**) complex and HCl as a byproduct. These two latter compounds react further, thus generating the binuclear complex **2** (by means of reaction **G**) and confirming the cyclic process proposed above.

$$2\,[Pt_2(\mu\text{-}SH)_2(P\cap P)_2]Cl_2\ (\mathbf{3}\text{-}Cl_2) \rightarrow [Pt_3(\mu_3\text{-}S)_2(P\cap P)_3]Cl_2\ (\mathbf{7}\text{-}Cl_2) + [Pt(SH)_2(P\cap P)]\ (\mathbf{4}) + 2\,HCl \quad (\mathbf{L})$$

The experimental data obtained in the titration of **1**, as well as **4**, with $HClO_4$ (Table 1) compare very well with those obtained with HCl, the only differences being due to the lower coordinating ability of the ClO_4^- counterion. As shown in Scheme 2, the addition of the first equivalent of $HClO_4$ to **1** leads to the immediate formation of the monoprotonated species **2**-ClO_4. Subsequent additions of $HClO_4$ cause the latter species to evolve to **4**, with the concomitant formation of the corresponding trinuclear complexes **7**-$(ClO_4)_2$, which, unlike **4**, do not react further under the present experimental conditions. As with the titration with HCl, it has not been possible to detect the transient diprotonated complexes **3**-$(ClO_4)_2$. Direct titration of **4** with $HClO_4$, has allowed us to verify that they evolve into the initial complexes **2**-ClO_4, and thus to reconfirm the cyclic nature of the protonation process of the $\{Pt_2S_2\}$ core in **1**. However, as the ClO_4^- counterion prevents the generation of analogues of **6**, the only dead end of the cycle is the formation of **7**-$(ClO_4)_2$. Detection of **7b**-$(ClO_4)_2$ requires a greater excess of acid than **7a**-$(ClO_4)_2$, which is easily observed in the titration of either **1a** or **4a** with $HClO_4$. The dependence of the ease of formation of the trinuclear species with the phosphine ligand, (greater stability for dppe than for dppp), compares well with the results obtained in the titration with HCl.

Theoretical study of the reaction pathway followed by the $[Pt_2(\mu\text{-}S)_2(P\cap P)_2]$ ($P\cap P$ = dppe, dppp) complexes in the presence of HCl: We have performed theoretical calculations to evaluate the thermodynamic feasibility of the proposed reactions (**A** – **L**) corresponding to the evolution of the $\{Pt_2S_2\}$ core in the presence of HCl. In addition to the energetic picture of the aforementioned reactions, and to the relative stabilities of the species involved, this study provides an insight into the structural features of the compounds involved, some of them not well characterized. In the calculations, we have modeled dppe and dppp real ligands by $H_2P(CH_2)_2PH_2$ (dhpe) and $H_2P(CH_2)_3PH_2$ (dhpp), respectively. To obtain realistic values of the reaction energies, the solvent has been taken into account in the calculations. The reason for proceeding in this way is that in some of the considered reactions the charges of reactants and products are not the same, the process entailing a net charge creation or annihilation. In these cases solvent effects on the thermodynamics of the reaction are dramatic. For instance, reaction **A** (charge of reactants 0, charge of products +1 and −1) is computed to be slightly exothermic in solution (~ -4.5 kcal mol^{-1}) but it is extremely endothermic in the gas phase ($\sim +82$ kcal mol^{-1}). The effect is much lower when the charges of reactants and products remain the same. For instance, ΔE values of approximately -7.5 kcal mol^{-1} and -9.5 kcal mol^{-1} are computed for reaction **E** in the gas phase and solution, respectively. To obtain a global picture of all the processes considered, solvent effects have been included in all the reactions. Thus, all the reported values have been obtained in acetonitrile as solvent ($\varepsilon = 36.64$) by means of the polarizable continuum model (PCM). Accordingly, the reaction energies (ΔE) for reactions **A** – **L** have been calculated (Table 3). From these values, it is possible to obtain the relative energy per "$\{Pt_2\}$" unit for all the species involved from $[Pt_2(\mu\text{-}S)_2(P\cap P)_2]$ (taken as the zero of energy) to $[Pt_3(\mu_3\text{-}S)_2(P\cap P)_3]^{2+}$ (Table 4), and to establish the energy profile for the whole process (Figure 1). Energies obtained with dhpe and dhpp ligands are very similar (see Table 3), and thus, only the values for dhpe are represented in Figure 1.

Table 3. Theoretical evaluation of energetic changes (ΔE) accompanying the proposed reactions pathways **A** – **L**. All energies are in kcal mol^{-1}.

	Reactions	ΔE	
		dhpe	dhpp
A	**1** + HCl → **2**-Cl	−4.7	−4.5
B	**2**-Cl + HCl → **3**-Cl_2	+17.2	+15.9
C	**3**-Cl_2 → 2 **5**	−41.5	−41.2
D	**3**-Cl_2 → **4** + **6**	−39.5	−39.1
E	**4** + HCl → **5** + H_2S	−9.1	−9.8
F	**5** + HCl → **6** + H_2S	−7.1	−7.7
G	2 **4** + HCl → **2**-Cl + 2 H_2S	+6.1	+5.6
H	2 **5** → **2**-Cl + HCl	+24.3	+25.2
I	**2**-Cl + **6** → **7**-Cl_2 + HCl	+17.8	+18.8
J	**2**-Cl + **5** → **7**-Cl_2 + H_2S	+10.7	+11.1
K	**2**-Cl + **4** + HCl → **7**-Cl_2 + 2 H_2S	+1.6	+1.4
L	2 **3**-Cl_2 → **7**-Cl_2 + **4** + 2 HCl	−38.9	−36.2

Table 4. Relative energy per dimer $\{Pt_2\}$ for compounds involved in the proposed reactions. The energy for complexes $[Pt_2(\mu\text{-}S)_2(P\cap P)_2]$ is arbitrarily taken to zero. All energies are in kcal mol^{-1}.

Compounds	Relative energy	
	dhpe	dhpp
1	0.0	0.0
2-Cl	−4.7	−4.5
3-Cl_2	+12.5	+11.4
2 **5**	−29.0	−29.7
4 + **6**	−27.0	−27.6
5 + **6**	−36.1	−37.4
2 **6**	−43.2	−45.1
5 + **4**	−19.9	−19.9
2 **4**	−10.8	−10.2
1/2 **4** + 1/2 **7**-Cl_2	−6.9	−6.7

In the overall process depicted in Scheme 1 can be considered as being formed by three steps: 1) protonation of the

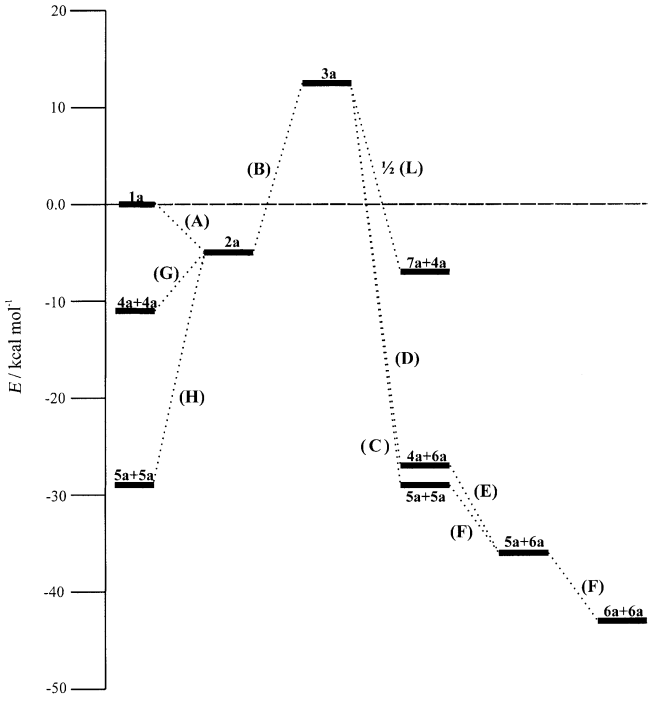

Figure 1. Energy profile for the reaction pathway of $[Pt_2(\mu\text{-}S)_2(dhpe)_2]$ with HCl in acetonitrile as solvent. Reactions are shown from left (reagents) to right (products).

bimetallic $\{Pt_2S_2\}$ core, which includes the addition of the first and second proton to the sulfido bridges; 2) cleavage of the bimetallic $\{Pt_2S_2\}$ core yielding various monometallic species, and their subsequent evolution by reaction with HCl; and 3) formation of trimetallic species either from dinuclear species alone or from a combination of mononuclear and dinuclear complexes.

1) Protonation of the $\{Pt_2S_2\}$ core: The two consecutive additions of H^+ to the sulfido bridges of $[Pt_2(\mu\text{-}S)_2(P\cap P)_2]$ have very different consequences. In the first protonation (reaction **A**), stable mixed (μ-S)(μ-SH)-bridged complexes are formed in a slightly exothermic ($\sim$5 kcal mol^{-1}) reaction, in agreement with the isolation, and in some cases X-ray characterization, of such compounds with Pt[11],[13] and Ni.[14] In contrast, the second protonation step (reaction **B**) is highly endothermic, indicating very unstable diprotonated complexes. We have checked the true minimum nature of the highly unstable diprotonated species by means of vibrational analysis. No imaginary frequencies are found for species **3**, thus confirming their nature as unstable reaction intermediates. Accordingly, the diprotonated complex could only be synthesized by using a large excess of protic acid. Notwithstanding this, owing to the cleavage of the $\{Pt_2(SH)_2\}$ ring (see below), no $[Pt_2(\mu\text{-}SH)_2(P\cap P)_2]^{2+}$ species has been isolated or detected in solution. The very difficult diprotonation of $[Pt_2(\mu\text{-}S)_2(P\cap P)_2]$, also found in $[Ni_2(\mu\text{-}S)_2(P\cap P)_2]$ complexes,[14] is consistent with the acidic nature of the sulfhydryl proton-sulfur bond. The thermodynamic instability of the diprotonated species is a key factor that justifies the sequence of reactions taking place in steps 2 and 3, leading to far more stable compounds.

The main structural parameters of optimized binuclear complexes, together with the X-ray structure of the parent experimental compounds, are given in Table 5.

Structural trends in edge-sharing binuclear d^8 complexes with X and XR bridges have recently been analyzed.[15] A characteristic structural parameter for complexes having $\{M_2(\mu\text{-}X)_2\}$ cores is the dihedral angle θ that describes the degree of folding of the M_2X_2 ring. This angle is $\sim$135° in compounds $[Pt_2(\mu\text{-}S)_2(P\cap P)_2]$, and small variations, of less than 2°, are found for all isomers of $[Pt_2(\mu\text{-}S)(\mu\text{-}SH)(P\cap P)_2]^+$.

Table 5. Calculated and X-ray-determined parameters for bimetallic and trimetallic complexes with $\{(P_2Pt)_n(\mu\text{-}S)_2\}$ cores.

Compound[a]	Pt···Pt	S···S	Pt–S	Pt–S_H	Pt-P_S	Pt–P_{SH}	S-Pt-S	Pt-S-Pt	Pt-S_H-Pt	P-Pt-P	θ	Reference[b]
$[(dhpe)_2Pt_2(\mu\text{-}S)_2]$	3.307	3.213	2.399	–	2.299	–	84.1	87.1	–	86.6	136.3	calcd
$[(dhpp)_2Pt_2(\mu\text{-}S)_2]$	3.293	3.222	2.406	–	2.294	–	84.1	86.4	–	95.6	134.4	calcd
$[(dppe)_2Pt_2(\mu\text{-}S)_2]$ (NILDAN)	3.292	3.134	2.350	–	2.245	–	83.7	88.9	–	86.2	140.2	[2f]
$[(dppp)_2Pt_2(\mu\text{-}S)_2]$	3.235	3.101	2.340	–	2.254	–	83.0	87.5	–	94.7	134.8	[6]
$[(Ph_2pyP)_2Pt_2(\mu\text{-}S)_2]$ (YIJNEK)	3.355	3.004	2.327	–	2.277	–	80.4	99.6	–	103.0	180.0	[5d]
$[(dhpe)_2Pt_2(\mu\text{-}S)(\mu\text{-}SH)]^+$	3.326	3.244	2.389	2.465	2.338	2.279	83.8	88.2	84.8	86.1	134.2	calcd: *exo*
$[(dhpe)_2Pt_2(\mu\text{-}S)(\mu\text{-}SH)]^+$	3.351	3.160	2.394	2.449	2.336	2.279	81.5	88.8	86.3	86.1	132.0	calcd: *endo*
$[(dhpp)_2Pt_2(\mu\text{-}S)(\mu\text{-}SH)]^+$	3.375	3.239	2.394	2.468	2.335	2.283	83.5	89.6	86.2	94.1	137.1	calcd: *exo*
$[(dhpp)_2Pt_2(\mu\text{-}S)(\mu\text{-}SH)]^+$	3.409	3.162	2.399	2.452	2.333	2.285	81.4	90.6	88.1	93.9	136.0	calcd: *endo*
$[(dppe)_2Pt_2(\mu\text{-}S)(\mu\text{-}SH)]^+$	3.350	3.057	2.341	2.371	2.261	2.244	80.9	91.4	89.9	85.7	138.3	[11]
$[(dppp)_2Pt_2(\mu\text{-}S)(\mu\text{-}SH)]^+$	3.237	3.004	2.344	2.353	2.262	2.260	79.5	87.4	86.9	93.3	127.4	[11]
$[(Ph_3P)_4Pt_2(\mu\text{-}S)(\mu\text{-}SH)]^+$ (QIDPUO)[c]	3.340	2.976	2.342	2.342	2.284	2.284	78.9	91.0	91.0	99.0	135.0	[13b]
$[(dhpe)_2Pt_2(\mu\text{-}SH)_2]^{2+}$	3.519	3.331	–	2.468	–	2.318	84.9	–	91.0	85.2	150.2	calcd: *exo*
$[(dhpe)_2Pt_2(\mu\text{-}SH)_2]^{2+}$	3.550	3.285	–	2.463	–	2.319	83.6	–	92.2	85.0	150.3	calcd: *anti*
$[(dhpp)_2Pt_2(\mu\text{-}SH)_2]^{2+}$	3.536	3.319	–	2.472	–	2.319	84.3	–	91.3	92.2	149.7	calcd: *exo*
$[(dhpp)_2Pt_2(\mu\text{-}SH)_2]^{2+}$	3.558	3.281	–	2.468	–	2.320	83.3	–	93.2	91.4	153.2	calcd: *anti*
$[(dhpe)_3Pt_3(\mu\text{-}S)_2]^{2+}$	3.257	3.118	2.443	–	2.312	–	78.3	83.6	–	85.5	120.0	calcd
$[(dhpp)_3Pt_3(\mu\text{-}S)_2]^{2+}$	3.272	3.112	2.448	–	2.312	–	78.9	83.9	–	92.9	120.0	calcd
$[(dppe)_3Pt_3(\mu\text{-}S)_2]^{2+}$ (CENRAO)	3.118	3.063	2.364	–	2.248	–	80.8	82.6	–	86.1	120.0	[2e]
$[(dppe)_3Pt_3(\mu\text{-}S)_2]^{2+}$ (PAHSOQ)	3.121	3.064	2.365	–	2.248	–	80.8	82.6	–	85.8	120.0	[18a]
$[(dppp)_3Pt_3(\mu\text{-}S)_2]^{2+}$ (**7b**)	3.130	3.024	2.357	–	2.301	–	79.8	83.2	–	93.1	120.0	*this work*
$[(PhMe_2P)_6Pt_3(\mu\text{-}S)_2]^{2+}$ (CIXRUW)	3.157	3.016	2.366	–	2.269	–	79.2	83.7	–	98.9	120.0	[18b]

[a] S and S_H indicate the sulfur atoms of sulfido and thiol groups, Pt–P_S are Pt–P lengths *trans* to SH groups. [b] For experimental compounds, if available, refcode of Cambridge Structural Database is given. [c] Hydrogen atoms are disordered between the two *endo* bridging sulfur atoms.

However, when both bridges are thiol groups, $[Pt_2(\mu\text{-}SH)_2(P\cap P)_2]^{2+}$, more planar rings are obtained ($\theta = 150^\circ$), with the concomitant lengthening of the Pt···Pt distance. These changes in the degree of bending are responsible for the variations on the bond angles about the sulfur bridges.[16] Two conformations, which differ in the *endo* or *exo* orientation of the thiol proton with respect the hinged Pt_2S_2 ring,[16] have been calculated for $[Pt_2(\mu\text{-}S)(\mu\text{-}SH)(P\cap P)_2]^+$. Isomer *endo* becomes most stable when the solvent effect is introduced, but with an energy difference of only 0.4 kcal mol^{-1}. Unfortunately, hydrogen atoms have not been located in the crystal structures, precluding a comparison with the calculated structures. For complexes $[Pt_2(\mu\text{-}SH)_2(P\cap P)_2]^{2+}$, the *syn-exo* conformation is found to be $\sim$1 kcal mol^{-1} more stable than the *bent-anti* one. Protonation of sulfido bridges lengthens Pt–S bonds, and Pt–S_H lengths (thiol bridge, $\sim$2.47 Å) are always longer than those of the Pt–S (sulfido bridge, $\sim$2.40 Å). The difference can be also observed in experimental compounds.[6] These variations in Pt–S/S_H lengths are reflected in the Pt–P lengths by a *trans* influence, and values of 2.28 Å and 2.32 Å are obtained for Pt–P_{SH} and Pt–P_S, *trans* to the thiol and sulfido group, respectively. The very elongated Pt–S_H bond in the diprotonated species is worth mentioning as it is consistent with the presence of weakened Pt–S bonds, a factor that facilitates its cleavage.

A major difference between the dhpe and dhpp phosphines is found in the bite P-Pt-P angle of the complexes. Despite the diversity of compounds calculated, dhpp complexes always have P-Pt-P angles greater than those with dhpe, with differences varying between 6° and 9° for analogous compounds. Whereas calculated dhpe complexes present bite angles in a range of 85 – 87°, compounds having dhpp ligand appear more flexible, with values of 91 – 96°. Experimental complexes with related chelating diphosphines show the same tendency.[6] We conclude that the presence of dppe or dppp terminal diphosphine does not significantly affect the thermodynamics of the protonation steps.

An interesting point for $[Pt_2(\mu\text{-}S)(\mu\text{-}SH)(P\cap P)_2]^+$ complexes, related to the acidic character of the SH proton, is the possibility of SH···S hydrogen bonding. We studied this aspect in a recent communication. In addition to the presence of weak hydrogen bonding, for **2a** and **2b** we reported the first evidence of a fast S–H···S proton transfer in a transition metal system.[11]

2) Cleavage of the {Pt_2S_2} core: Two processes, which lead to different monometallic compounds, can be envisaged for the disintegration of the $\{Pt_2(\mu\text{-}SH)_2\}$ skeleton. If the two Pt–S bonds of the same platinum atom are broken, two different products, $[PtCl_2(P\cap P)]$ and $[Pt(SH)_2(P\cap P)]$ are formed (reaction **D**). In contrast to this, the rupture of one Pt–S bond from each moiety affords two mononuclear $[PtCl(SH)(P\cap P)]$ complexes (reaction **C**). Both processes are very exothermic and have similar reaction energies (around -40 kcal mol^{-1}). It can be expected that both processes take place simultaneously, and thus that species **4** – **6** are all present in solution. It is clear from Figure 1 that the driving force for the disintegration of the bimetallic species is the thermodynamic stability of the mononuclear compounds formed from the cleavage of the $\{Pt_2S_2\}$ core.

The experimental study shows that protonation of the SH ligands in **4** and **5** is followed by their subsequent replacement by Cl^- anions, leading to **6** as the final products. The substitution of the first SH^- by one Cl^- is favored by $\sim$9 kcal mol^{-1} (reaction **E**), and the second replacement by $\sim$7 kcal mol^{-1} (reaction **F**). The monometallic dichloride compounds are very stable, unreactive species, and their formation appears as a dead end in Figure 1. When $HClO_4$ is used as the source of protons, only dithiol complexes can be formed, due to the non-coordinating nature of the perchlorate anions.

Experimental data evidencing formation of bimetallic $[Pt_2(\mu\text{-}S)(\mu\text{-}SH)(P\cap P)_2]^+$ complexes from monometallic species show that the disintegration/formation of the $\{Pt_2S_2\}$ core is a cyclic process. Calculations indicate that the presence of $[Pt(SH)_2(P\cap P)]$ compounds is crucial for the cyclic character of this process. Such species are the less stable monometallic compounds, and $[Pt_2(\mu\text{-}S)(\mu\text{-}SH)(P\cap P)_2]^+$ complexes are found to be only 6 kcal mol^{-1} above two $[Pt(SH)_2(P\cap P)]$ molecules (reaction **G**). Formation of **2** from the direct dimerization of two $[PtCl(SH)(P\cap P)]$ monomers (reaction **H**) appears less plausible, given the high endothermicity of the reaction ($\sim$24 kcal mol^{-1}). As this process involves the formation of HCl, its removal with a base should facilitate the thermodynamically unfavored reaction **H**, as reported for related compounds in the presence of ternary amines.[5d] Consequently, the presence of NaSH, and its reaction with HCl, probably accounts for the experimental evolution of **6** to **2**. In an acidic medium, a more favorable pathway from **5** to **2** would probably require prior exchange of Cl^- by SH^- ligands in **5** to afford **6** and **4**, the latter evolving to **2** (reaction **G**).

Structural data for optimized monometallic complexes and related experimental compounds are presented in Table 6. As for the bimetallic complexes, a good agreement with the X-ray determined data is found. It is worth mentioning that the SH^- ligands have a stronger *trans* influence than Cl^- on the Pt–P bonds, as reflected in the Pt–P_S bonds, which are 0.05 Å longer than the Pt–P_{Cl}. The S···S distance in monometallic dithiol complexes is longer than in bimetallic or trimetallic due to greater S-Pt-S angles (Table 5 and Table 6). The optimized geometries show an increase in the P-Pt-P angles for the monometallic compounds when SH^- is replaced by Cl^-.

3) Generation of trimetallic species: Several possible pathways can be proposed to account for the generation of trimetallic complexes, among which trimolecular reactions can be excluded for kinetic reasons. Accordingly, on the basis of a bimolecular reaction, the following reaction mechanisms are possible: i) combination of two bimetallic complexes to give one trimetallic and one monometallic species and, ii) one bimetallic species reacts with a monometallic complex.

The reaction of two diprotonated dimers $[Pt_2(\mu\text{-}SH)_2(P\cap P)_2]^{2+}$ (**3**) to afford $[Pt_3(\mu_3\text{-}S)_2(P\cap P)_3]^{2+}$ (**7**) and $[Pt(SH)_2(P\cap P)]$ (**4**) (reaction **L**) is highly favored, mainly because of the diprotonated dimer's high energy. The mononuclear complex **4** can regenerate the $\{Pt_2S_2\}$ core by reaction

Table 6. Calculated and X-ray-determined geometrical parameters for $[PtX_2(P\cap P)]$ (X = Cl or SH) complexes. Some selected experimental compounds retrieved from Cambridge Structural Database are also shown.

Compound[a]	Pt–Cl	Pt–S	$Pt–P_{Cl}$[b]	$Pt–P_S$[b]	P-Pt-P	X-Pt-X	Reference[b]
[(dhpe)$PtCl_2$]	2.399	–	2.253	–	88.4	96.2	calcd
[(dhpp)$PtCl_2$]	2.408	–	2.257	–	98.5	95.9	calcd
[(dppe)$PtCl_2$] (BOFVIB)	2.348	–	2.208	–	86.2	90.2	[29]
[(dpype)$PtCl_2$] (WIXGIT)	2.354	–	2.210	–	86.2	90.8	[30]
[(dppe)$PtCl_2$] (DEBXUD)	2.355	–	2.227	–	86.8	89.1	[31]
[(dcype)$PtCl_2$] (WANHOI)	2.366	–	2.223	–	87.7	89.2	[32]
[(dtbpe)$PtCl_2$] (CBPTCB)	2.366	–	2.261	–	89.4	86.7	[33]
[(dtbpe)$PtCl_2$] (CBPEPT)	2.369	–	2.264	–	89.4	86.3	[33]
[(dppp)$PtCl_2$] (FONKOI)	2.362	–	2.232	–	91.6	88.4	[34]
[(dtbpp)$PtCl_2$] (BUPRPT)	2.360	–	2.282	–	99.1	83.2	[35]
mean values[c]	*2.352 ± 14*	–	*2.229 ± 23*	–	*94.6 ± 6.1*	*88.4 ± 1.8*	
[(dhpe)PtCl(SH)]	2.400	2.388	2.255	2.308	87.0	92.3	calcd
[(dhpp)PtCl(SH)]	2.407	2.395	2.256	2.313	95.4	91.8	calcd
[$(Ph_3P)_2PtCl(SAr)_2$] (PINDAR)	2.334	2.320	2.249	2.286	96.6	90.5	[36]
[(dhpe)$Pt(SH)_2$]	–	2.404	–	2.305	86.2	92.8	calcd
[(dhpp)$Pt(SH)_2$]	–	2.412	–	2.304	94.0	92.0	calcd
[(dppe)$Pt(SH)_2$] (**4a**)	–	2.350	–	2.251	86.2	87.6	this work
[(dppp)$Pt(SH)_2$] (**4b**)	–	2.356	–	2.270	91.2	86.2	this work
[(dppe)$Pt(SPh)_2$] (KIXGUT)	–	2.350	–	2.249	86.1	99.2	[37]
[(dppe)$Pt(SPy)_2$] (FOQPOQ)	–	2.358	–	2.263	85.7	82.7	[38]
[(dppe)$Pt(SPip)_2$] (KURMIT)	–	2.373	–	2.260	86.0	93.5	[39]
[$(Ph_3P)_2Pt(SH)_2$] (DTHLPT01)	–	2.343	–	2.255	97.0	86.8	[9b]
[$(Ph_3P)_2Pt(SAr)_2$] (PINDEV)	–	2.361	–	2.323	97.7	93.7	[36]

[a] For experimental compounds, phosphine (R = 2-py for dpype, R = Cy for dcype, R = *t*Bu for dtbpe, dtbpp) and monodentate ligands (SPy = 2-thiopyridinato, SPip = 4-thio-2-methyl-pyperidine, SAr = 2,4,6-tris(isopropyl)phenylthiolate anions) are as indicated; in most cases the refcode for the compound in the Cambridge Structural Database is provided. [b] $Pt–P_{Cl}$ and $Pt–P_S$ are Pt–P lengths *trans* to Cl and SH groups. [c] Mean and standard deviation of sample for 178 fragments of 166 refcodes found in a search on Cambridge Structural Database.

G, as shown above, although this reaction is competitive with the substitution of SH^- by Cl^- if the acid added is HCl. Complexes **3** are very unstable species, having two different ways of evolving towards stable products: disintegration (reactions **C** and **D**) or recombination (reaction **L**). Thus, it is not surprising that different behavior is observed, depending on factors such as the presence or absence of coordinating conjugate bases or the nature of the solvent.

Alternatively, $[Pt_2(\mu\text{-}S)(\mu\text{-}SH)(P\cap P)_2]^+$ may react with a monometallic complex (**4**, **5** or **6**) to form $[Pt_3(\mu_3\text{-}S)_2(P\cap P)_3]^{2+}$. This reaction is very plausible for **4** (reaction **K**), with a reaction energy of less than 2 kcal mol^{-1}, but the energy increases when the chloro complexes [PtCl(SH)(P∩P)] (**5**) or $[PtCl_2(P\cap P)]$ (**6**) are considered (~11 and ~18 kcal mol^{-1}, respectively). So reactions **I** and **J** are far less probable for the formation of the trimetallic complex (**7**) in acidic medium.

The high value calculated for the energy of reaction **I** agrees with the experimental data that complexes **2a**-Cl and **6a** do not react among themselves, and thus their combination cannot be a possible source of complex **7a**-Cl_2. It is clear that while the evolution of **2** in the presence of $HClO_4$ leads exclusively to the trimer **7**, in the presence of HCl, the formation of **7** competes with that of highly stable and inactive chloro complexes **6**.

One aspect of the formation of trimetallic $[Pt_3(\mu_3\text{-}S)_2(P\cap P)_3]^{2+}$ complexes that is not well reproduced by our calculations is the effect of the diphosphine ligand. Formation of these species is easier with dppe than with dppp. Our calculations give very similar ΔE values for both dhpe and dhpp throughout the corresponding reaction pathways. It seems reasonable to propose that the observed experimental differences are due to kinetic rather than thermodynamic factors.[17]

Structural data for $[Pt_3(\mu_3\text{-}S)_2(P\cap P)_3]^{2+}$ complexes have been presented in Table 5, where bimetallic compounds have been included for the sake of comparison. The Pt–S distances in the trimetallic species show similar values, which are intermediate between the Pt–SH and Pt–S distances found in dinuclear complexes with a $\{Pt_2S_2\}$ core. Furthermore, the bending angles of 120° in the trinuclear species imply shorter Pt···Pt distances than in the dinuclear analogues.[1]

Spectroscopic and structural characterization of the platinum complexes formed during the acid titration of $[Pt_2(\mu\text{-}S)_2P\cap P_2]$ (P∩P = dppe, dppp): The identification of the complexes formed in the evolution of $[Pt_2(\mu\text{-}S)_2(P\cap P)_2]$ (P∩P = dppe (**1a**), dppp (**1b**)) in the presence of HCl and $HClO_4$, which was monitored by $^{31}P\{^1H\}$ NMR data, required knowledge of the spectroscopic features of the species involved in this process. To this end, the synthesis and structural and spectroscopic characterization of complexes **4a**, **4b** and **7b**-$(PF_6)_2$ was undertaken; that of **1a** and **1b**,[2f,6] as well as their corresponding precursors, **6a** and **6b**,[12] and of **7a**-Cl_2,[2e] were already known. Within this context, the synthesis and X-ray crystal structures of **2a**-ClO_4 and **2b**-ClO_4 were also achieved. As variable-temperature $^{31}P\{^1H\}$ NMR studies in solutions containing **2a** or **2b** were indicative of an unprecedented intramolecular SH···S proton transfer in both cations, all these results have been anticipated in the form of a communication.[11] Main NMR and ESI MS parameters for complexes **1**, **2**, **4**, **6** and **7** are summarized in Table 2. Our unsuccessful attempts to isolate the doubly-protonated spe-

cies, **3a** and **3b**, are consistent with the absence of fully characterized sulfide-bridged analogous platinum complexes with other phosphine ligands.

As regards the monoprotonated complexes **2**, they were easily identified on the basis of the $^{31}P\{^{1}H\}$ NMR parameters at room temperature, where the four phosphorus nuclei become equivalent in solution, and easily characterized by ESI MS (Table 2). On the other hand, the ESI MS-monitored reaction of the isolated **2a**-ClO_4 and **2b**-ClO_4 with acid gave peaks at *m*/*z* 626.3 and 640.0, respectively, which could be initially assigned as $[\mathbf{2a}+H]^{2+}$ and $[\mathbf{2b}+H]^{2+}$. These observations, together with the fact that the intensity of both peaks increased when more acid was added to these mixtures, would be consistent with the formation of the corresponding doubly-protonated species, **3a** and **3b**, despite their elusive nature under usual laboratory conditions. Interestingly, we have observed peaks with the same *m*/*z* values (626.2 and 640.1) in the ESI MS spectra of **4a** and **4b**. In these species, the loss of one SH^- ligand accounts for the formation of the $[Pt(SH)(P\cap P)]^+$ fragment, whose mass exactly coincides with half of that of $[Pt_2(\mu\text{-}SH)_2(P\cap P)_2]^{2+}$. Accordingly, the mass spectral data obtained after adding acid to **2a**-ClO_4 and **2b**-ClO_4 would also be compatible with the formation of the corresponding $[Pt(SH)(P\cap P)]^+$ fragment, and thus the existence of the diprotonated cations, **3a** and **3b**, under ESI MS conditions is inconclusive evidence.

Complexes **4** have been characterized in the solid state by X-ray diffraction, as well as in solution. The $^{31}P\{^{1}H\}$ NMR spectra of **4**, unlike all the dinuclear and trinuclear platinum complexes involved in the evolution of **1** in the presence of acid, display a first-order pattern (Table 2). Concerning the signal corresponding to the protons of the SH groups in **4a** and **4b**, it appears as a false triplet, due to $^{2}J_{H,Pt}$ coupling, in both $^{1}H\{^{31}P\}$ NMR spectra, but it shows different patterns in the ^{1}H NMR spectra. Thus, for complex **4b**, containing the dppp ligand, it shows the $^{3}J_{H,P}$ coupling involving only the phosphorus atom *trans* to hydrogen, while for **4a**, with dppe, both $^{3}J_{H,P}$ couplings to P_{trans} and P_{cis} can be observed (Figure 2). These variations could be attributed to the different geometric constraints imposed by the diphosphine ligands, as the average P-Pt-S angle for adjacent P and S atoms is about 2° greater in **4a** than in **4b** (see below).

In addition, complex **7b**-$(PF_6)_2$ has been characterized in the solid state by X-ray diffraction, as well as in solution. Although it has been obtained by a different procedure from that followed for its analogue **7a**-Cl_2,[2e] the structures of **7a** and **7b** in the solid state compare well, as described below. Similarly, interpretation of the $^{31}P\{^{1}H\}$ NMR spectra of **7b** in solution requires consideration of second-order effects, as already reported for **7a**,[2e] whose spin system has facilitated the computer simulation and thus determination of the $^{1}J_{P,Pt}$, $^{2}J_{Pt,Pt}$ $^{3}J_{P,Pt}$ and $^{4}J_{P,P}$ coupling constants given in Table 2.

Molecular structures: Complexes **4a** and **4b** are structurally related as they both consist of mononuclear $[Pt(SH)_2(P\cap P)]$ discrete molecules ($P\cap P$ = dppe (**4a**), Figure 3, or dppp (**4b**), Figure 4), devoid of crystallographic symmetry elements. In the case of **4a**, there is also one CH_2Cl_2 molecule for each formula unit. The listing of the main geometric parameters for **4a** and **4b** appears in Table 7. In both **4a** and **4b**, the platinum atom has square planar coordination; the twist between the PtS_2 and PtP_2 planes is 7.2° (**4a**) or 3.4° (**4b**). In neither case could the hydrogen atoms of the SH groups be located, probably because they are rotationally disordered, having no hydrogen bond interactions.

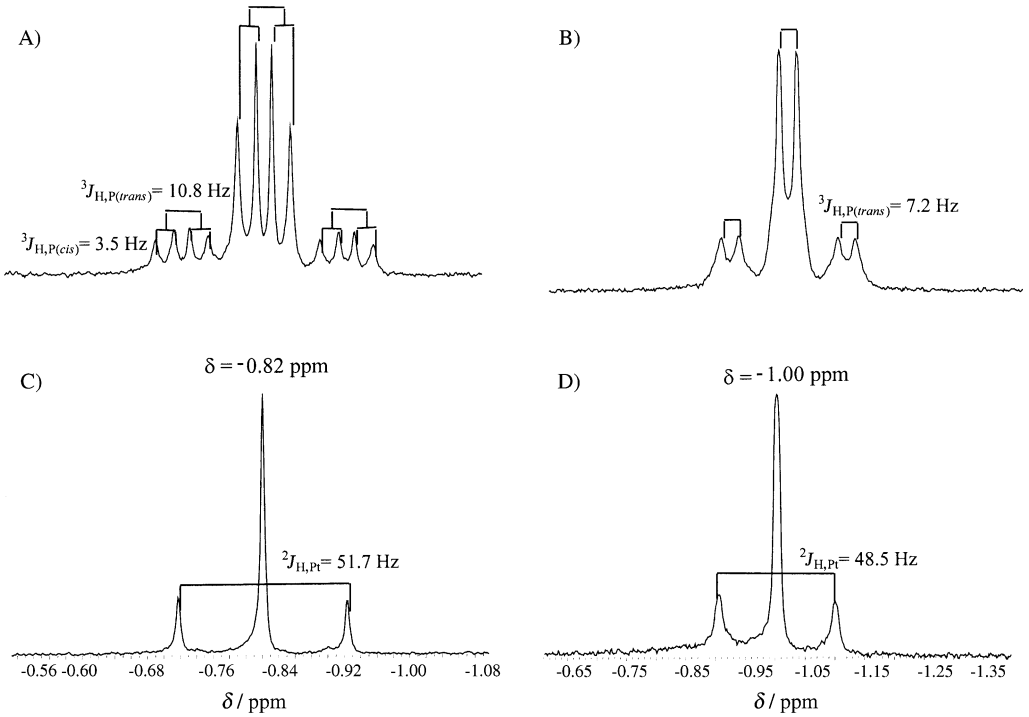

Figure 2. ^{1}H NMR signals corresponding to the SH groups in **4a** (A) and **4b** (C). $^{1}H\{^{31}P\}$ NMR signals corresponding to the SH groups in **4a** (B) and **4b** (D).

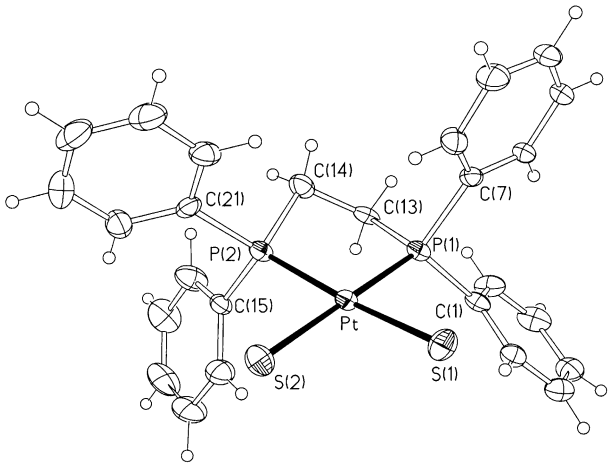

Figure 3. Structure of complex **4a**, with 50% probability displacement ellipsoids and selected atom labels.

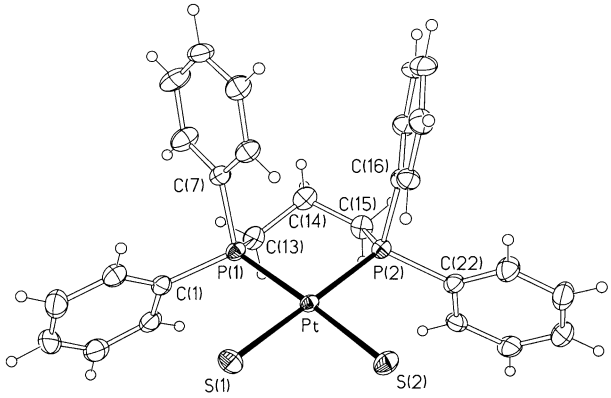

Figure 4. Structure of complex **4b**, with 50% probability displacement ellipsoids and selected atom labels.

Table 7. Selected bond lengths [Å] and angles [°] for compounds **4a** and **4b**.

	4a	**4b**
P–S(1)	2.3528(12)	2.3561(10)
Pt–S(2)	2.3469(14)	2.3553(10)
Pt–P(1)	2.2545(12)	2.2668(10)
Pt–P(2)	2.2478(12)	2.2730(10)
S(1)-Pt-S(2)	87.60(5)	86.16(4)
P(1)-Pt-P(2)	86.16(5)	91.16(4)
Pt-P(1)-C(13)	107.89(18)	114.08(13)
Pt-P(2)-C(14/15)	105.3(3)	117.02(14)

Comparison of **4a** and **4b** with the only other reported analogue for which structural parameters are available, $[Pt(SH)_2(PPh_3)_2]$,[9b] shows that the three structures have remarkable similarities. Obviously, they differ in the P-Pt-P angles (86.2 (**4a**), 91.2 (**4b**), and 97.0° for PPh_3 ligands), but these differences have no significant effect on the structural parameters involving the $Pt(SH)_2$ fragment (S-Pt-S angles are 87.6, 86.2, and 86.8°, respectively). Concerning the Pt(P∩P) moieties in **4a** and **4b**, their geometric features are in good concordance with those observed, respectively, in $[PtCl_2(dppe)]$ (**6a**) and $[PtCl_2(dppp)]$ (**6b**)[12] as well as in related species such as $[Pt_2(\mu\text{-}S)_2(P\cap P)_2]$ (P∩P = dppe (**1a**) or dppp (**1b**)),[2d,6] $[Pt_2(\mu\text{-}S)(\mu\text{-}SH)(P\cap P)_2]^+$ (P∩P = dppe (**2a**) or dppp (**2b**)),[11] and $[Pt_3(\mu_3\text{-}S)_2(P\cap P)_3]^{2+}$ (P∩P = dppe (**7a**)[2e] or dppp (**7b**)). As expected, the S-Pt-S angle, and thus the S–S length, in the $Pt(SH)_2$ fragment of the three mononuclear species are greater than those in the $\{Pt_2S_2\}$ rings of the dinuclear (**2**) or trinuclear complexes (**7**).

Complex **7b**-$(PF_6)_2$ consists of discrete trinuclear $[Pt_3(\mu_3\text{-}S)_2(dppp)_3]^{2+}$ cations (Figure 5) and PF_6^- anions, held together by electrostatic interactions. Main geometric parameters for **7b** are given in Table 8. The C_{3h} crystallographic

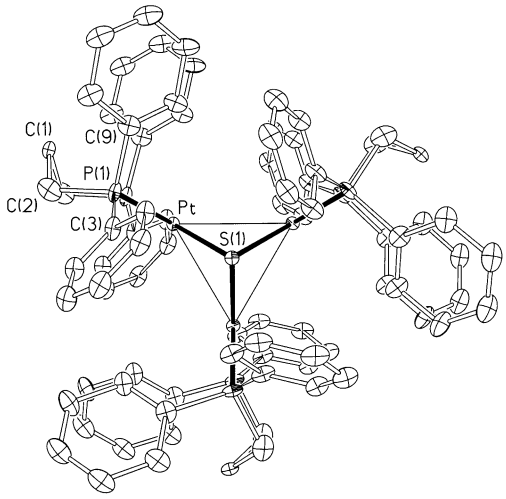

Figure 5. Structure of the complex cation **7b**, viewed along the threefold rotation axis, with 10% probability displacement ellipsoids and selected atom labels.

Table 8. Selected bond lengths [Å] and angles [°] for compound **7b**-$(PF_6)_2$.

Pt(1)–S(1)	2.357(7)	Pt(1)–P(1)	2.301(8)
S(1)-Pt(1)-S(1A)	79.8(4)	S(1)-Pt(1)-P(1)	93.5(3)
S(1)-Pt(1)-P(1A)	173.7(3)	P(1)-Pt(1)-P(1A)	93.1(5)
Pt(1)-S(1)-Pt(1B)	83.2(3)	Pt(1)-P(1)-C(2)	121(2)
Pt(1)···Pt(1A)	3.131(3)	θ	120.0

Symmetry operations for equivalent atoms: A: $x, y, 1-z$; B: $1-y, x-y, z$.

symmetry of the cation, the regular trigonal bipyramid geometry of the central Pt_3S_2 unit, and the square planar coordination of the platinum atoms in the three sulfur-linked PtS_2P_2 units are the main features of this structure, and compare well with those of the $[Pt_3(\mu_3\text{-}S)_2(dppe)_3]^{2+}$ (**7a**) analogue, already reported.[2e] By extending the structural comparison not only to the three other examples containing a $\{Pt_3(\mu_3\text{-}S)_2\}$ core,[2e,18] but also to complexes with a $\{Pt_3(\mu_3\text{-}X)_2\}$ core (X = Se, Te),[19] it is noteworthy that they all show significant similarities and that, among them all, the Pt_3S_2 core in complex **7b** has the highest crystallographic symmetry.

Concluding Remarks

Detailed study of the evolution of $[Pt_2(\mu\text{-}S)_2(P\cap P)_2]$ (P∩P = dppe or dppp) in the presence of protic acids, HCl or $HClO_4$,

confirms the outstanding nucleophilicity of the sulfide ligands in the $\{Pt_2S_2\}$ core. Experimental observations and theoretical calculations have allowed us to propose a cascade of sequential reactions triggered by the protonation of the stable monoprotonated $[Pt_2(\mu\text{-}S)(\mu\text{-}SH)(P\cap P)_2]^+$ complexes. This second protonation first involves disintegration of the $\{Pt_2S_2\}$ ring, and, eventually, regeneration of the monoprotonated dinuclear complex. Formation of complexes $[Pt(SH)_2(P\cap P)]$ is the keystone for the cyclical nature of the overall processes. The complexes $[PtCl_2(P\cap P)]$ and $[Pt_3(\mu_3\text{-}S)_2(P\cap P)_3]^{2+}$ do not react any further and thus are responsible for the cycles' dead end. Remarkably, the reaction pathways can be directed by controlling i) the concentration and nature of the protic acid (ie, the coordinative features of the conjugate anion); ii) the chelating diphosphine ligands, each having a particular bite angle; and iii) the polarity of the solvent used. Overall, while the richness of the chemistry of $[Pt_2(\mu\text{-}S)_2(P\cap P)_2]$ metalloligands was not unexpected, their tremendous versatility in the presence of protic acids had not been known up to that point. The cyclical nature of the latter processes, as well as the relevance of complexes containing the metal-SH fragment in the hydrodesulfurization processes, provides additional interest to the present findings with respect to their potential catalytic applications.

Experimental Section

Materials and methods: All manipulations were carried out at room temperature under an atmosphere of pure dinitrogen, and conventionally dried and degassed solvents were used throughout. These were Purex Analytical Grade from SDS. Metal complexes of formula $[PtCl_2(P\cap P)]$, $P\cap P$ = dppe (**6a**) or dppp (**6b**), were prepared according to published methods.[12] The synthesis of $[(P\cap P)Pt(\mu\text{-}S)_2Pt(P\cap P)]$, $P\cap P$ = dppe (**1a**) or dppp (**1b**), has already been reported.[2f,6]

Elemental analyses were performed on a Carlo-Erba CHNS EA-1108 analyzer. Analytical data for the carbon content in **4a** and **7b**-$(PF_6)_2$ deviate from calculated values, as already found in related complexes.[6],[11] Notwithstanding this, both complexes have been fully characterized by NMR, ESI MS and X-ray diffraction data. ^{1}H, ^{13}C{^{1}H} and ^{31}P{^{1}H} NMR spectra were recorded from samples in $(CD_3)_2SO$ solution at room temperature, using a Bruker AC250 spectrometer. ^{13}C and ^{1}H chemical shifts are relative to $SiMe_4$, and ^{31}P chemical shifts to external 85 % H_3PO_4. The ^{31}P{^{1}H} NMR spectrum of $[Pt_3(\mu_3\text{-}S)_2(dppp)_3]^{2+}$ was simulated on a Pentium-200 computer using the gNMR V4.0.1 program by P. H. M. Budzelaar from Cherwell Scientific Publishing.[20] The ESI MS measurements were performed on a VG Quattro Micromass Instrument. Experimental conditions were as follows: 10 μL of sample was injected at 15 μL min^{-1}; capillary-counter electrode voltage, 4.5 kV; lens-counter electrode voltage, 1.0 kV; cone potential, 55 V; source temperature, 90 °C; *m*/*z* range, 300 to 1600. The carrier was a 1:1 mixture of acetonitrile and water containing 1 % formic acid. In the case of the $[Pt_2(\mu\text{-}S)(\mu\text{-}SH)(P\cap P)_2]^+$ cations, **2a** and **2b**, the ESI MS measurements were carried out at different concentrations of formic acid (1 %, 10 % and 20 %).

Titration of $[Pt_2(\mu\text{-}S)_2(P\cap P)_2]$ ($P\cap P$ = dppe, 1a, or dppp, 1b) and $[Pt(SH)_2P\cap P]$ ($P\cap P$ = dppe, 4a or dppp, 4b) with HCl or $HClO_4$: In order to analyze the course of the reaction of **1a**, **1b**, **4a** and **4b** with HCl or $HClO_4$, controlled amounts of a concentrated or 2 M solution of acid were added to a solution of 10 mg of the corresponding pure compound in 5 mL of CH_3CN. The different solutions were evaporated to dryness, and the ^{31}P NMR spectra in $[D_6]$DMSO were recorded. When the amount of acid added impaired the evaporation to dryness, adding water to the previously concentrated solution precipitated the product.

Evolution with time of a solution of $[Pt_2(\mu\text{-}S)(\mu\text{-}SH)(P\cap P)_2]ClO_4$ ($P\cap P$ = dppe, 2a-ClO_4, or dppp, 2b-ClO_4) in the presence of HCl or $HClO_4$: $HClO_4$ (conc., 30 μL, 0.34 mmol) or HCl (conc., 25 μL, 0.30 mmol) was added to a solution of **2a**-ClO_4 or **2b**-ClO_4 (100 mg, 0.074 mmol **2a**-ClO_4, 0.072 mmol **2b**-ClO_4) in 50 mL of CH_3CN, CH_3OH, $(CH_3)_2CO$ or CH_2Cl_2. This solution was monitored for one week by taking one aliquot every 24 h, evaporating it to dryness and recording the ^{31}P NMR spectrum in $[D_6]$DMSO.

Reaction between $[Pt_2(\mu\text{-}S)(\mu\text{-}SH)(P\cap P)_2]ClO_4$ ($P\cap P$ = dppe, 2a-ClO_4, or dppp, 2b-ClO_4) and $[PtCl_2(P\cap P)]$ ($P\cap P$ = dppe, 6a or dppp, 6b): Solid **6a** or **6b** (50 mg, 0.075 mmol) was added to a solution of **2a**-ClO_4 or **2b**-ClO_4 (100 mg, 0.074 mmol **2a**-ClO_4, 0.072 mmol **2b**-ClO_4) in CH_3CN (50 mL), with stirring. The resulting suspension was stirred for one week and monitored by taking one aliquot every 24 h, evaporating it to dryness and recording the ^{31}P NMR spectrum in $[D_6]$DMSO. These data revealed that the reaction of **2a** with **6a**, as well as that of **2b** with **6b**, does not proceed under these experimental conditions.

Reaction between $[PtCl_2(P\cap P)]$ ($P\cap P$ = dppe, 6a or dppp, 6b) and $NaSH\cdot H_2O$ at a 1:1 molar ratio: $NaSH\cdot H_2O$ (11 mg, 0.150 mmol) was added to a suspension of **6a** or **6b** (100 mg, 0.150 mmol **6a**, 0.147 mmol **6b**) in benzene (50 mL). After 8 h of stirring, the final suspension was evaporated to dryness. The ^{31}P{^{1}H} NMR spectrum in $[D_6]$DMSO of the solid thus obtained showed the presence of the corresponding complexes of formulae $[Pt_2(\mu\text{-}S)(\mu\text{-}SH)(P\cap P)_2]Cl$ (**2a**-Cl or **2b**-Cl), and $[Pt(SH)_2(P\cap P)]$ (**4a** or **4b**) as a minor component. Alternatively, when the experiment was carried out using a fivefold excess of $NaSH\cdot H_2O$ (50 mg, 0.68 mmol), complexes **4a** or **4b** were obtained as major products and **1a** and **1b** as minor components. Formation of the latter can be attributed to the presence of sulfide as a minor impurity in commercial $NaSH\cdot H_2O$.

Synthesis of $[Pt(SH)_2(dppe)]$ (4a): $[PtCl_2(dppe)]$ (**6a**) (500 mg, 0.73 mmol) was added to a benzene solution (250 mL) of $NaSH\cdot H_2O$ (200 mg, 2.7 mmol) and the mixture stirred at room temperature for 8 h. The excess $NaSH\cdot H_2O$, the formed NaCl and the unreacted $[PtCl_2(dppp)]$ were filtered off. The filtrate was concentrated to 5 mL and the yellow solid was filtered and washed with diethyl ether. Yield 63 %; elemental analysis calcd (%) for $C_{26}H_{26}P_2PtS_2$: C 47.34, H 3.97, S 9.72; found: C 46.55, H 4.00, S 9.48. X-ray quality crystals of this compound were obtained by slow evaporation of a solution in CH_2Cl_2.

Synthesis of $[Pt(SH)_2(dppp)]$ (4b): Using the same procedure as that indicated for the previous compound, a yellow solid was obtained from the reaction of $[PtCl_2(dppp)]$ (**6b**) (500 mg, 0.75 mmol) with $NaSH\cdot H_2O$ (200 mg, 2.7 mmol) in a benzene solution (250 mL). Yield 59 %; elemental analysis calcd (%) for $C_{27}H_{28}P_2PtS_2\cdot C_6H_6$: C 52.72, H 4.56, S 8.53; found: C 52.93, H 4.84, S 7.93. Recrystallization in CH_2Cl_2 allowed isolation of yellow crystals.

Synthesis of $[Pt_3(\mu_3\text{-}S)_2(dppp)_3](PF_6)_2$, 7b-$(PF_6)_2$: $Na_2S\cdot 9H_2O$ (50 mg, 0.21 mmol) was added to a CH_3CN solution (25 mL) of $[PtCl_2(dppp)]$ (**6b**) (192 mg, 0.28 mmol) and KPF_6 (36 mg, 0.21 mmol) and the mixture stirred at room temperature for 24 h. These reaction conditions were chosen after monitoring the reaction by means of ^{31}P NMR, which allowed determination of the most appropriate reaction time for maximum yield. The NaCl and KCl formed were filtered off. The solvent was removed from the filtrate under vacuum, to yield the title compound as a yellow solid. Yield 75.0 %; elemental analysis calcd (%) for $C_{81}H_{78}F_{12}P_8Pt_3S_2$: C 44.70, H 3.61, S 2.95; found: C 43.89, H 3.60, S 2.94. Recrystallization of this compound from methanol gave colorless crystals suitable for X-ray diffraction.

CAUTION: The concentrated solutions of $HClO_4$ can give rise to explosive reactions. Concentrated $HClO_4$ should not make contact with dmso, because the reaction is very violent and exothermic.

X-ray crystallographic characterization: Crystal data for complexes **4a**, **4b** and **7b**-$(PF_6)_2$ are given in Table 9. All measurements were made at 160 K on a Bruker AXS SMART CCD diffractometer, with graphite-monochromated $Mo_{K\alpha}$ radiation (λ = 0.71073 Å). Cell parameters were refined from the observed positions of all strong reflections in the complete data sets. Absorption corrections were applied by inter-frame scaling procedures, based on redundant and symmetry-equivalent reflections.[21] The structures were solved by direct methods, and refined on all unique F^2 values, with anisotropic displacement parameters and constrained isotropic hydrogen atoms.[21] Hydrogen atoms could not be located on the SH ligands, and are probably rotationally disordered. Satisfactory refinement of the structure of **7b**-$(PF_6)_2$ was hampered by extensive disorder of the anions (modeled approximately by partial-occupancy sites for F atoms, the sum of the

Table 9. Crystallographic data for complexes **4a**, **4b** and **7b**-$(PF_6)_2$.

Complex	**4a** · CH_2Cl_2	**4b**	**7b**-$(PF_6)_2$
formula	$C_{26}H_{26}P_2PtS_2 \cdot CH_2Cl_2$	$C_{27}H_{28}P_2PtS_2$	$C_{81}H_{78}P_6Pt_3S_2(PF_6)_2$
M	744.5	673.6	2176.6
crystal system	orthorhombic	monoclinic	hexagonal
space group	$P2_12_12_1$	$P2_1/n$	$P62c$
a [Å]	9.7477(4)	12.9935(5)	16.774(5)
b [Å]	13.4951(6)	9.1308(4)	
c [Å]	21.0737(9)	21.2394(9)	19.025(4)
β [°]		91.997(2)	
V [Å^{-3}]	2772.2(2)	2518.33(18)	4636(2)
Z	4	4	2
ρ_{calcd} [g cm^{-3}]	1.784	1.777	1.559
μ [mm^{-1}]	5.54	5.88	4.76
reflections measured	22357	20755	23387
unique reflections	6412	5873	2101
R_{int}	0.037	0.039	0.097
parameters	308	290	186
R (F, $F^2 > 2\sigma$)	0.030	0.027	0.128
R_w (F^2, all data)	0.064	0.059	0.334
goodness of fit on F^2	1.10	1.04	1.22
max., min. electron density [e Å^{-3}]	1.80, −1.59	1.33, −1.35	6.04, −2.31

occupancies being constrained to 6 per anion; all P–F lengths are reasonable, but the angles are essentially meaningless and the anions are probably extensively rotationally disordered). An ambiguous space group assignment (many candidate space groups could fit the observed diffraction data approximately equally well, but no sensible ordered structure could be obtained in any lower-symmetry space group), and partial racemic twinning; the refinement was assisted by restraints on ligand geometry and atomic displacement parameters, and the gross structure of the trinuclear cation is unambiguously established.

CCDC-206306 (**4a**), CCDC-206307 (**4b**), and CCDC-206305 (**7b**-$(PF_6)_2$) contain the supplementary crystallographic data for this paper. These data can be obtained free of charge at www.ccdc.cam.ac.uk/conts/retrieving.html (or from the Cambridge Crystallographic Data Centre, 12 Union Road, Cambridge CB21EZ, UK; fax: (+44) 1223-336-033; or e-mail: deposit@ccdc.cam.ac.uk).

Computational details: Calculations were performed using the GAUSSIAN98 series of programmes.[22] Geometry optimizations were done in the full potential energy surface, without restrictions, using density functional theory (DFT) with the hybrid B3LYP functional.[23]. In the case of the most unstable species, vibrational analysis were performed to characterize them as minima. Effective core potentials (ECP) and their associated double-ξLANL2DZ basis set were used for the platinum, phosphorus, sulfur and chlorine atoms,[24] supplemented by an extra *d*-polarization in the case of P, S and Cl.[25] The 6–31G basis set was used for the C and H atoms.[26] Solvent effects were taken into account by means of PCM calculations,[27] using standard options of PCM and cavity keywords.[22] Energies were calculated with acetonitrile ($\varepsilon = 36.64$) as solvent, keeping the geometry optimized for the isolated species (single-point calculations). We have already used this approach in the study of the reactions of $[L_2Pt(\mu\text{-}S)_2PtL_2]$ with CH_2Cl_2.[6]

Structural analysis: Collection of structural data was carried out using the Cambridge Structural Database (Version 5.23).[28]

Acknowledgement

Financial support from the Ministerio de Ciencia y Tecnología of Spain (projects BQU2001–1976 and BQU2002–04110-CO2–02) is gratefully acknowledged. This research was partially supported by the Improving Human Potential Programme, Access to Research Infrastructures under contract HPRI-1999-CT-000071, Access to CESCA and CEPBA Large-Scale Facilities established between the European Community and CESCA-CEPBA. RMB is indebted to the Universitat Autònoma de Barcelona for a pre-doctoral scholarship.

[1] S.-W. A. Fong, T. S. A. Hor, *J. Chem. Soc. Dalton Trans.* **1999**, 639, and references therein.
[2] Selected recent references: a) S.-W. A. Fong, W. T. Yap, W. Teck, J. J. Vittal, W. Henderson, T. S. A. Hor, *J. Chem. Soc. Dalton Trans.* **2002**, 1826; b) Z. Li, Z.-H. Loh, K. F. Mok T. S. A. Hor, *Inorg. Chem.* **2000**, *39*, 5299; c) Z. Li, X. Xu, S. Khoo, K. F. Mok, T. S. A. Hor, *J. Chem. Soc. Dalton Trans.* **2000**, 2901; d) H. Liu, C. Jiang, J. S. L. Yeo, K. F. Mok, L. K. Liu, T. S. A. Hor, Y. K. Yan, *J. Organomet. Chem*. **2000**, *595*, 276; e) M. Capdevila, Y. Carrasco, W. Clegg, R. A. Coxall, P. González-Duarte, A. Lledós, J. A. Ramírez, *J. Chem. Soc. Dalton Trans.* **1999**, 3103; f) M. Capdevila, Y. Carrasco, W. Clegg, P. González-Duarte, A. Lledós, J. Sola, G. Ujaque, *Chem. Commun.* **1998**, 597.
[3] J. Chatt, D. M. P. Mingos, *J. Chem. Soc. A* **1970**, 1243.
[4] R. Ugo, G. La Monica, S. Cenini, A. Segre, F. Conti, *J. Chem. Soc. A* **1971**, 522.
[5] a) R. R. Gukathasan, R. H. Morris, A. Walker, *Can. J. Chem*. **1983**, *61*, 2490; b) M. Zhou, C. F. Lam, K. F. Mok, P.-H. Leung, T. S. A. Hor, *J. Organomet. Chem.* **1994**, *476*, C32; c) A. Shaver, R. D. Lai, P. H. Bird, W. Wickramasinghe, *Can. J. Chem*. **1985**, *63*, 2555; d) V. W.-W. Yam, P. Kok-Yan, K.-K. Cheung, *J. Chem. Soc. Chem. Commun.* **1995**, 267; e) M. Zhou, P.-H. Leung, K. F. Mok, T. S. A. Hor, *Polyhedron* **1996**, *15*, 1737.
[6] R. Mas-Ballesté, M. Capdevila, P. A. Champkin, W. Clegg, R. A. Coxall, A. Lledós, C. Mégret, P. González-Duarte, *Inorg. Chem.* **2002**, *41*, 3218.
[7] H. Li, G. B. Carpenter, D. A. Sweigart, *Organometallics* **2000**, *19*, 1823.
[8] R. J. Angelici, *Acc. Chem. Res.* **1988**, *21,* 391.
[9] a) M. S. Morton, R. N. Lachicotte, D. A. Vicic, W. D. Jones, *Organometallics* **1999**, *18*, 227; b) R. Vicente, J. Ribas, X. Solans, G. Germain, *An. Quim. Ser. B* **1986**, *82*, 47.
[10] A. Shaver, M. El-Khateeb, A.-M. Lebuis, *Angew. Chem.* **1996**, *108*, 2510; *Angew. Chem. Int. Ed. Engl*. **1996**, *35*, 2362.
[11] G. Aullón, M. Capdevila, W. Clegg, P. González-Duarte, A. Lledós, R. Mas-Ballesté, *Angew. Chem.* **2002**, *114*, 2900; *Angew. Chem. Int. Ed.* **2002**, *41*, 2776.
[12] M. P. Brown, R. J. Puddephatt, M. Rashidi, K. R. Seddon, *J. Chem. Soc. Dalton Trans.* **1977**, 951.
[13] a) S.-W. A. Fong, W. T. Yap, J. J. Vittal, T. S. A. Hor, W. Henderson, A. G. Oliver, C. E. F. Rickard, *J. Chem. Soc. Dalton Trans.* **2001**, 1986; b) S.-W. A. Fong, J. J. Vittal, W. Henderson, T. S. A. Hor, A. G. Oliver, C. E. F. Rickard, *Chem. Commun.* **2001**, 421.
[14] S. S. Oster, R. J. Lachicotte, W. D. Jones, *Inorg. Chim. Acta* **2002**, *330*, 118.

[15] G. Aullón, G. Ujaque, A. Lledós, S. Alvarez, *Chem. Eur. J.* **1999**, *5*, 1391.
[16] G. Aullón, A. Lledós, S. Alvarez, *Inorg. Chem.* **2000**, *39*, 906.
[17] The effect of the bite angle on reactivity has been recently reviewed: a) P. Dierkes, P. W. N. M. van Leeuwen, *J. Chem. Soc., Dalton Trans.* **1999**, 1519; b) P. W. N. M. van Leeuwen, P. C. J. Kamer, J. N. H. Reek, P. Dierkes, *Chem. Rev.* **2000**, *100*, 2741; c) P. C. J. Kamer, P. W. N. M. van Leeuwen, J. N. H. Reek, *Acc. Chem. Res.* **2001**, *34*, 895.
[18] a) M. J. Pilkington, A. M. Z. Slawin, D. J. Williams, J. D. Woollins, *J. Chem. Soc. Dalton Trans.* **1992**, 2425; b) G. W. Bushnell, K. R. Dixon, R. Ono, A. Pidcock, *Can. J. Chem.* **1984**, *62*, 696; c) Z. Li, H. F. Mok, A. S. Batsanov, J. A. K. Howard, T. S. A. Hor, *J. Organomet. Chem.* **1999**, *575*, 223.
[19] a) A. L. Ma, J. B. Thoden, L. F. Dahl, *J. Chem. Soc. Chem. Commun.* **1992**, 1516; b) K. Matsumoto, M. Ikuzawa, S. Ooi, *Inorg. Chim. Acta* **1994**, *217*, 129; c) R. Oliunkaniem, R. S. Laitinen, M. Ahlgren, *J. Organomet. Chem.* **2000**, *595*, 232.
[20] P. H. M. Budzelaar, *gNMR (V4.01)*; Cherwell Scientific Publishing Ldt.: Oxford, 1997.
[21] SMART, SAINT, SADABS and SHELXTL software; Bruker AXS Inc.: Madison, WI, 2001.
[22] M. J. Frisch, G. W. Trucks, H. B. Schlegel, G. E. Scuseria, M. A. Robb, J. R. Cheeseman, V. G. Zakrzewski, J. A. Montgomery, R. E. Stratmann, J. C. Burant, S. Dapprich, J. M. Millam, A. D. Daniels, K. N. Kudin, M. C. Strain, O. Farkas, J. Tomasi, V. Barone, M. Cossi, R. Cammi, B. Mennucci, C. Pomelli, C. Adamo, S. Clifford, J. Ochterski, G. A. Petersson, P. Y. Ayala, Q. Cui, K. Morokuma, D. K. Malick, A. D. Rabuck, K. Raghavachari, J. B. Foresman, J. Cioslowski, J. V. Ortiz, B. B. Stefanov, G. Liu, A. Liashenko, P. Piskorz, I. Komaromi, R. Gomperts, R. L. Martin, D. J. Fox, T. Keith, M. A. Al-Laham, C. Y. Peng, A. Nanayakkara, M. Challacombe, P. M. W. Gill, B. Johnson, W. Chen, M. W. Wong, J. L. Andres, C. Gonzalez, M. Head-Gordon, E. S. Replogle, J. A. Pople, Gaussian98 (Revision A.7), Gaussian Inc., Pittsburgh, PA, **1998**.
[23] a) A. D. Becke, *J. Chem. Phys.* **1993**, *98*, 5648; b) C. Lee, W. Yang, R. G. Parr, *Phys. Rev. B* **1988**, *37*, 785.
[24] a) P. J. Hay, W. R. Wadt, *J. Chem. Phys.* **1985**, *82*, 299; b) P. J. Hay, W. R. Wadt, *J. Chem. Phys.* **1985**, *82*, 270.
[25] A. Höllwarth, M. Böhme, S. Dapprich, A. W. Ehlers, A. Gobbi, V. Jonas, K. F. Köhler, R. Stegman, A. Veldkamp, G. Frenking, *Chem. Phys. Lett.* **1993**, *208*, 237.
[26] W. J. Hehre, R. Ditchfield, J. A. Pople, *J. Chem. Phys.* **1972**, *56*, 2257.
[27] a) J. Tomasi, M. Persico, *Chem. Rev.* **1994**, *94*, 2027; b) C. Amovilli, V. Barone, R. Cammi, E. Cancès, M. Cossi, B. Mennucci, C. S. Pomelli, J. Tomasi, *Adv. Quantum Chem.* **1998**, *32*, 227.
[28] F. H. Allen, O. Kennard, *Chem. Des. Autom. News* **1993**, *8*, 31.
[29] D. H. Farrar, G. Ferguson, *J. Cryst. Spectrosc. Res.* **1982**, *12*, 465; B. Bovio, F. Bonati, G. Banditelli, *Gazz. Chim. Ital.* **1985**, *115*, 613.
[30] N. D. Jones, K. S. MacFarlane, M. B. Smith, R. P. Schutte, S. J. Rettig, B. R. James, *Inorg. Chem.* **1999**, *38*, 3956.
[31] L. M. Engelhardt, J. M. Patrick, C. L. Raston, P. Twiss, A. H. White, *Aust. J. Chem.* **1984**, *37*, 2193.
[32] J. T. Mague, M. J. Fink, C. A. Recatto, *Acta Crystallogr. Sect. C* **1993**, *49*, 1176.
[33] M. Harada, Y. Kai, N. Yasuoka, N. Kasai, *Bull. Chem. Soc. Jpn.* **1976**, *49*, 3472.
[34] G. B. Robertson, W. A. Wickramasinghe, *Acta Crystallogr. Sect. C* **1987**, *43*, 1694.
[35] M. Harada, Y. Kai, N. Yasuoka, N. Kasai, *Bull. Chem. Soc. Jpn.* **1979**, *52*, 390.
[36] Q. Chen, F. Boeheim, J. Dabrowiak, J. Zubieta, *Inorg. Chim. Acta* **1994**, *216*, 83.
[37] W. Gou-Wei, H. Zhi-Ying, H. Mao-Chun, L. Han-Qin, *Jiegou Huaxue J. Struct. Chem.* **1991**, *10*, 159.
[38] T. S. Lobana, R. Verma, G. Hundal, A. Castiñeiras, *Polyhedron* **2000**, *19*, 899.
[39] M. Capdevila, W. Clegg, P. González-Duarte, B. Harris, I. Mira, J. Sola, I. C. Taylor, *J. Chem. Soc. Dalton Trans.* **1992**, 2817.

Received: March 24, 2003 [F4983]

